nzsee
NEW ZEALAND SOCIETY FOR EARTHQUAKE ENGINEERING

Influence of ground motion orientation on predicted seismic compression

R.A. Green & M. Bahrampouri
Department of Civil and Environmental Engineering, Virginia Tech, Blacksburg, VA, USA.

ABSTRACT

Seismic compression is the accrual of contractive volumetric strain in unsaturated or partially saturated sandy soils during earthquake shaking and has caused significant distress to overlying and nearby structures. The phenomenon can be well-characterized by load-dependent, interaction macro-level fatigue theories, which means that the nature of the accumulation of volumetric strain is a function of the absolute amplitude and sequencing of pulses in the loading function. One model that captures this behavior and that can be used to predict seismic compression is the expanded Byrne cyclic shear-volumetric strain coupling model. However, one potential implication of the load-dependent, interaction macro-level fatigue behaviour is that ground motion orientation will influence predicted settlements. To examine the significance of this, the seismic compression that occurred at the Kashiwazaki-Kariwa Nuclear Power Plant (KKNPP) site during the 2007, M_w6.6 Niigata-ken Chuetsu-oki, Japan, earthquake is analyzed using the expanded Byrne model. The horizontal motions recorded at the site by a down-hole array during this event are rotated in 5° increments and the predicted settlements due to seismic compression are computed. The predicted settlements range from 12.3 to 16.1 cm, with a geometric mean of the values for various orientations being 13.8 cm. These results are in general accord with the post-earthquake field observations and highlight the sensitivity of predicted magnitude of the seismic compression to ground motion orientation.

1 INTRODUCTION

Seismic compression is the accrual of contractive volumetric strain in unsaturated or partially saturated sandy soils during earthquake shaking (i.e., vibration-induced settlement) (Stewart et al. 2004). Seismic compression has occurred in several earthquakes and can significantly distress overlying and nearby structures. Adopting the terminology used for liquefaction triggering procedures, with slight modification, seismic compression evaluation procedures can be broadly classified as “simplified” and “non-simplified”. In the context used herein, simplified approaches use relatively simple ground motion parameterization to characterize the seismic demand (e.g., effective shear strain, γ_{eff}, and number of equivalent strain cycles,

$n_{eq\gamma}$), while non-simplified procedures use more detailed characterization of seismic demand (e.g., shear strain, γ, time histories computed using numerical site response analyses).

To the authors' knowledge, Finn and Byrne (1976) were the first to propose a non-simplified approach for evaluating seismic compression. In their procedure the seismic demand is quantified in terms of shear strain time histories acting on horizontal planes at various depths within the soil profile, computed by numerical site response analyses. Increments in volumetric strain are then computed using a model proposed by Martin et al. (1975) that relates shear and volumetric strains. As discussed in Green and Lee (2006) and Lasley et al. (2016), the Martin et al. (1975) model is a load-dependent, interaction macro-level fatigue model, as is the subsequently proposed variant by Byrne (1991) (i.e., the nature of the accumulation of volumetric strain is a function of the amplitude of the load and is influenced by previous loading, e.g., Kaechele 1963). One potential implication of the load-dependent, interaction macro-level fatigue behaviour is that ground motion orientation influences the predicted settlements. Hence the objective of the study presented herein is to examine the significance of this. Towards this end, the seismic compression that occurred at the Kashiwazaki-Kariwa Nuclear Power Plant (KKNPP) site during the 2007, M_w6.6 Niigata-ken Chuetsu-oki, Japan, earthquake is analyzed using an expanded form of the Byrne shear strain-volumetric strain coupling model (Green and Jiang 2020; Jiang et al. 2020).

In the following, the expanded Byrne shear strain-volumetric strain coupling model is briefly presented, followed by background information on the seismic compression case history from the 2007, M_w6.6 Niigata-ken Chuetsu-oki, Japan, earthquake. Next, a parametric study is presented wherein the horizontal motions recorded by the down-hole array at the case history site are rotated in 5° increments and used in conjunction with the non-simplified form of the expanded Byrne model to predict settlements due to seismic compression.

2 EXPANDED BYRNE MODEL

Byrne (1991) proposed the following variant of the Martin et al. (1975) cyclic shear-volume strain coupling non-simplified model to estimate volumetric strains in dry sands:

$$\varepsilon_v = \sum_i \left(\Delta\varepsilon_{v,1/2}\right)_i \tag{1a}$$

where ε_v = accumulated volumetric strain in percent at the end of loading; and $(\Delta\varepsilon_{v,1/2})_i$ = increment in volumetric strain in percent at the end of the i^{th} half-shear strain cycle of loading having an amplitude γ_i. For earthquake loading, γ_i is typically taken as the peak shear strain between two zero crossings in the shear strain time history (e.g., Green and Terri 2005). $(\Delta\varepsilon_{v,1/2})_i$ is computed as:

$$\left(\Delta\varepsilon_{v,1/2}\right)_i = 0.5 \cdot (\gamma_i - \gamma_{tv}) \cdot C_1 \cdot exp\left[-C_2 \frac{\varepsilon_{vi}}{(\gamma_i - \gamma_{tv})}\right] \tag{1b}$$

where C_1 and C_2 are material-specific calibration parameters; ε_{vi} is the volumetric strain in percent at the beginning of the i^{th} load increment; γ_{tv} = threshold shear strain in percent; and γ_i is in percent. Based on the analysis of the laboratory data for Crystal Silica Sand No. 2 from Silver and Seed (1971) and Seed and Silver (1972), Byrne (1991) provided expressions to estimate C_1 and C_2:

$$C_1 = 7{,}600 \cdot Dr^{-2.5} \tag{2a}$$

$$C_2 = \frac{0.4}{C_1} \tag{2b}$$

where Dr is the relative density of the sand in percent.

As detailed in the Jiang et al. (2020), the Byrne (1991) model can be written in the alternative form:

$$\varepsilon_{vi} = -ln(\prod_i t_i) \cdot \frac{(\gamma_i - \gamma_{tv})}{C_2} \quad (3a)$$

where:

$$t_i = \begin{cases} e^{-0.5 \cdot C_1 \cdot C_2} & if\ i = 1 \\ (t_{i-1})^{t_{i-1}} & if\ i > 1 \end{cases} \quad (3b)$$

and ε_{vi} is in percent and corresponds to the end of the i^{th} load increment having amplitude γ_i, and both γ_i and γ_{tv} are in percent. If the seismic demand is expressed in terms of γ_{eff} and $n_{eq\gamma}$, Equation 3 can be written in simplified form:

$$\varepsilon_v = -ln\left(\prod_{i=1}^{2 \cdot n_{eq\gamma}} t_i\right) \cdot \frac{(\gamma_{eff} - \gamma_{tv})}{C_2} \quad (4)$$

where ε_v is the volumetric strain at the end of shaking, γ_{eff} is typically taken as 0.65 the peak shear strain at the depth of interest (e.g., Dobry et al. 1982), and $n_{eq\gamma}$ is estimated using empirical correlations (e.g., Green and Lee 2006; Lee and Green 2017).

Comparison of Equation 4 with laboratory data and with simplified equations proposed by Duku et al. (2008) and Yee et al. (2014) dictates that the Byrne model be expanded. Specifically, the simplified form of the Byrne model can be expanded to:

$$\varepsilon_v = -ln\left(\prod_{i=1}^{2 \cdot n_{eq\gamma}} t_i\right) \cdot \frac{(\gamma_{eff} - \gamma_{tv})^{C_3}}{C_2} \quad (5)$$

and to:

$$\left(\Delta\varepsilon_{v,1/2}\right)_i = 0.5 \cdot (\gamma_i - \gamma_{tv})^{C_3} \cdot C_1 \cdot exp\left[-C_2 \frac{\varepsilon_{vi}}{(\gamma_i - \gamma_{tv})^{C_3}}\right] \quad (6)$$

for the non-simplified form. The calibration coefficients for Equations 3b and 5 (i.e., C_1, C_2, and C_3) are the same as those for Equation 6.

3 CASE HISTORY

3.1 Background

The main shock of the M_w6.6 Niigata-ken Chuetsu-oki, Japan, earthquake occurred on 16 July 2007. The event affected an ~100-km-wide area along the coastal regions of southwestern Niigata prefecture and triggered ground failures as far as the Unouma Hills, located in central Niigata approximately 50 km from the shore (Kayen et al. 2009). Of specific interest to this study is the seismic compression that occurred during this event at the Kashiwazaki-Kariwa Nuclear Power Plant (KKNPP) site (Yee et al. 2011). What makes this case history of particular value is that the motions at the site were recorded by a free-field downhole array (Service Hall Array, SHA) and the magnitude of the seismic compression was accurately determined to be ~10-20 cm from the settlement of soil around a vertical pipe housing one of the array seismographs.

Yee et al. (2011) performed a detailed site investigation and determined that the profile at the strong motion array consists of ~70 m of medium-dense sands overlying clayey bedrock and that the ground water table (gwt) is at a depth of ~45 m. Suspension logging and Standard Penetration Tests (SPT) with energy measurements were performed at the site, with the former providing small-strain shear and compression wave velocities (i.e., Vs and Vp, respectively). Additionally, laboratory tests were performed on disturbed and undisturbed samples to classify the soil, to determine index properties and shear strength of the soil, and to develop modulus reduction and damping (MRD) curves. The geologic log and instrument locations for the

SHA site are shown in Figure 1. Also, shown in this figure are the results SPT and suspension logging geophysical testing and some of their interpretation.

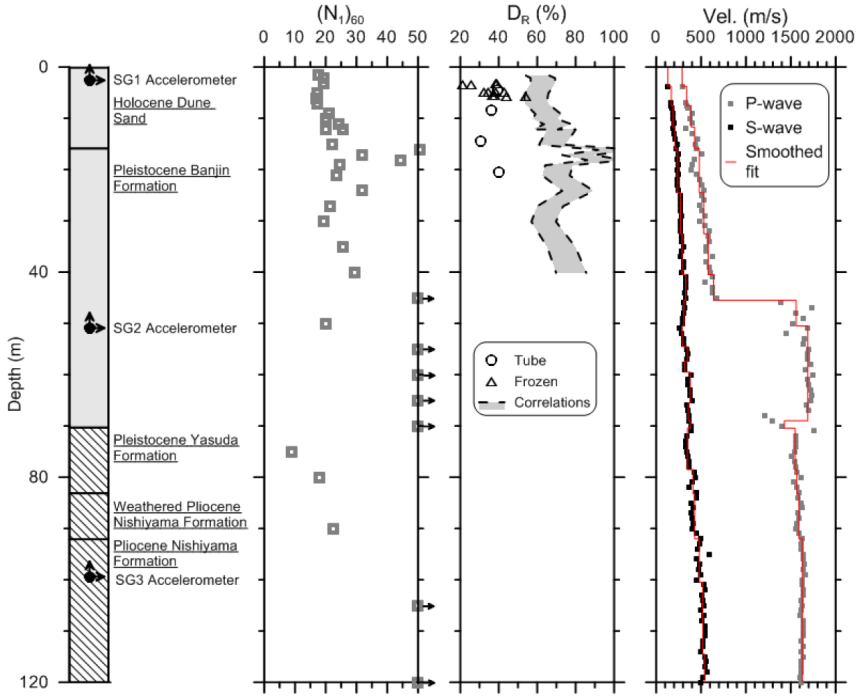

Figure 1: Geologic log for the SHA site including instrument locations and data SPT and suspension logging geophysical testing (Yee et al. 2011)

3.2 Expanded Byrne Model Calibration

Yee et al. (2011) performed a series of drained cyclic simple shear tests on samples from the KKNPP site and the results are used herein to develop relationships for the calibration parameters (i.e., C_1, C_2, and C_3) for the expanded Byrne model (i.e., Eqs. 5 and 6) for Dr ≈ 35% and 60%:

$$C_1 = K_{\sigma,\varepsilon} \cdot 1.28 \cdot e^{-0.019 \cdot Dr} \tag{7a}$$

$$K_{\sigma,\varepsilon} = \left(\frac{\sigma_v'}{P_a}\right)^{-0.29} \tag{7b}$$

$$C_2 = \frac{0.7864}{C_1} \tag{7c}$$

$$C_3 = 1.2 \tag{7d}$$

where Dr is in percent; P_a is atmospheric pressure in the same units as σ'_v; and σ'_v is the vertical effective stress at the depth of interest. Additionally, Yee et al. (2011) determined that γ_{tv} for the soil is ~0.03%. To compute σ'_v, the total unit weights (γ_t) of the soil listed in Table 1 were assumed.

Table 1: Assumed soil types and unit weights used in analysis (Motamed et al. 2016).

Depth range (m)	Soil type	Total unit weight, γ_t (kN/m^3)
0-4	Sand	16
4-45	Sand	17.75
45-70	Sand	20.8
70-99.4	Clay	20.8

Dr for the soil is estimated using the relationship (Skempton 1986):

$$Dr = 100 \cdot \sqrt{\frac{N_{1,60}}{C_d}} \tag{8}$$

where $N_{1,60}$ is the corrected SPT blow count, C_d is a soil-specific parameter, and Dr is in percent. Skempton (1986) recommended $C_d = 55$ for natural deposits of fine sand (with estimated Dr values using $C_d \approx 55$ shown as "Correlations" in Fig. 1). However, $C_d = 145$ is required to get the Dr values predicted using Equation 8 to match those determined from frozen samples and tube samples taken at the site (also shown in Fig. 1); accordingly, $C_d = 145$ is assumed herein.

3.3 Site Response Model Calibration

One-dimensional equivalent linear (EQL) site response analyses were performed for the site using the software Strata (Kottke and Rathje 2009) following the modeling details in Yee et al. (2011, 2013). The Menq (2003) modulus reduction and damping (MRD) curves are used to model the sandy soil above the gwt, with the Yee et al. (2013) strength-adjustment applied and a minimum damping of 5% used. To account for the influence of effective confining stress, the reference strain (γ_r) used in the Menq (2003) modulus reduction curves (i.e., curves of $(G/G_{max})_{\gamma eff}$ vs. γ_{eff}) were adjusted using:

$$\gamma_r = \gamma_{r,1} \cdot \left(\frac{\sigma'_o}{P_a}\right)^n \tag{9}$$

where σ'_o is the mean effective confining stress; P_a is in the same units as σ'_o; $\gamma_{r,1}$ is the reference strain for $\sigma'_o = 1$ atm; and n is an empirical soil-specific factor. Based on the MRD test data for sandy soils above the gwt from the KKNPP site, $\gamma_{r,1} = 0.0904$ and $n = 0.4345$ (Yee et al. 2013). No samples from below the gwt from the site were tested, and it is assumed that the $\gamma_{r,1}$ and n values proposed by Menq (2003) apply to sandy soils below the gwt: $\gamma_{r,1} = 0.0684$ and $n = 0.4345$. The Darendeli (2001) MRD curves were used for the relatively plastic soils and rock materials below 70 m. To compute σ'_o from the σ'_v values needed for Equation 7b, at rest lateral earth pressure coefficients for the various strata in the profile were obtained from Yee et al. (2011). Finally, the Vs profile used in the EQL analyses is shown in Figure 1.

4 PARAMETRIC STUDY

The unprocessed ground motions recorded by the SHA array were obtained from the Tokyo Electric Power Company (TEPCO) and were processed following the procedures detailed in Boore (2005), and Boore and Bommer (2005). This involved adding zero pads at the beginning and end of each record equal to $1.5 \cdot n'/f_c \cdot dt$, where $n' = 4$ (the high-pass filter order), f_c is the filter corner frequency, and dt is the sampling interval. An acausal high-pass filter was applied at the filter corner frequencies which were picked manually by comparing the signal with noise in frequency domain and visualizing the displacement. The same corner frequencies were used for all three components of motion recorded by a strong motion station during the event. The horizontal motions were oriented in the EW and NS directions, and those corresponding to a depth of 99.4 m were specified as "with-in" input motions in the EQL analyses.

The non-simplified expanded Byrne model (Eq. 6) calibrated using Equations 7 and 8 was used in conjunction with the shear strain time histories computed at the center of each of the Strata model layers above bedrock. The total settlement at the ground surface (S_T) at the site was then computed from the resulting ε_v values for each layer:

$$S_T = \sum_j \varepsilon_{v_j} \cdot \Delta z_j \tag{10}$$

where ε_{vj} is the volumetric strain in the j^{th} layer; and Δz_j is the thickness of the j^{th} layer.

Lasley and Green (2012) (also see Nie et al. 2017) proposed the values tabulated in Table 2 to relate seismic compression in soil subjected to geometric mean of the horizontal motions to that resulting from the soil being subjected to two horizontal components of motions simultaneously. The values listed in Table 2 are based on a series of numerical analyses with soil elements subjected to multidirectional motions, wherein the soil response was modeled using a reduced-order bounding surface hypoplasticity model (Li et al. 1992). Using Table 2 and assuming Dr ranges from 35% to 60% (Fig. 1 and Eq. 8), a factor of ~1.7 should be applied to the geometric mean of the settlement computed from the two horizontal components of motion for this event. Additionally, in a detailed, but somewhat limited, laboratory study, Pyke et al. (1975) examined the influence of vertical motions on seismic compression, where the vertical motions had peak ground accelerations (PGAs) ranging from 0.15g to 0.3g and acted in combination with horizontal motions. They found that the vertical motions can increase the seismic compression by 20% to 50%, relative to the seismic compression resulting from horizontal motions alone. Yee et al. (2011) accounted for vertical accelerations in predicting the magnitude of seismic compression at the KKNPP SHA site using an effective peak vertical acceleration of 0.4g for the event, which increases the predicted seismic compression by ~50% per Pyke et al. (1975) (i.e., $C_V = 1.5$).

Table 2: Correction Factor, C_{2D}, for Two-Dimensional Shaking (Lasley and Green 2012; also see Nie et al. 2017).

Dr (%)	**Moment Magnitude, M_w**		
($N_{1,60}$)	**5-6**	**6-7**	**7-8**
45 (9)	1.5	1.6	1.7
60 (17)	1.9	1.8	1.8
80 (30)	2	1.9	1.8
100 (46)	2	2.1	2.1

Assuming $C_{2D} = 1.7$ and $C_V = 1.5$, the predicted settlement using the non-simplified form of the expanded Byrne model for the EW and NS motions is ~12.3 cm. To assess the influence of the motion orientation of the magnitude of the predicted settlements due to seismic compression, the motions were rotated in 5° increments and the case history re-analyzed. The predicted settlements ranged from 12.3 to 16.1 cm, as shown in Figure 2. This range is in good accord with post-event observations at the KKNPP site (i.e., 10-20 cm). However, this relatively large variation in predicted settlements due to motion orientation highlights the importance of both the absolute amplitude and sequencing of pulses in the load history on predicted magnitude of seismic compression (i.e., the significance of the load-dependent, interaction macro-level fatigue behavior exhibited by the seismic compression phenomenon), which is commonly ignored in computation of $n_{eq\gamma}$ (e.g., Green and Terri 2005; Lee and Green 2017).

For the final prediction for this case history, the geometric mean of predicted magnitudes of seismic compression using the rotated motions is recommended, analogous to modern ground motion prediction equations (GMPEs) (e.g., Boore et al. 2006). Using this approach, the predicted settlement for this case history is ~13.8 cm, which is, again, in good accord with the post-event observations.

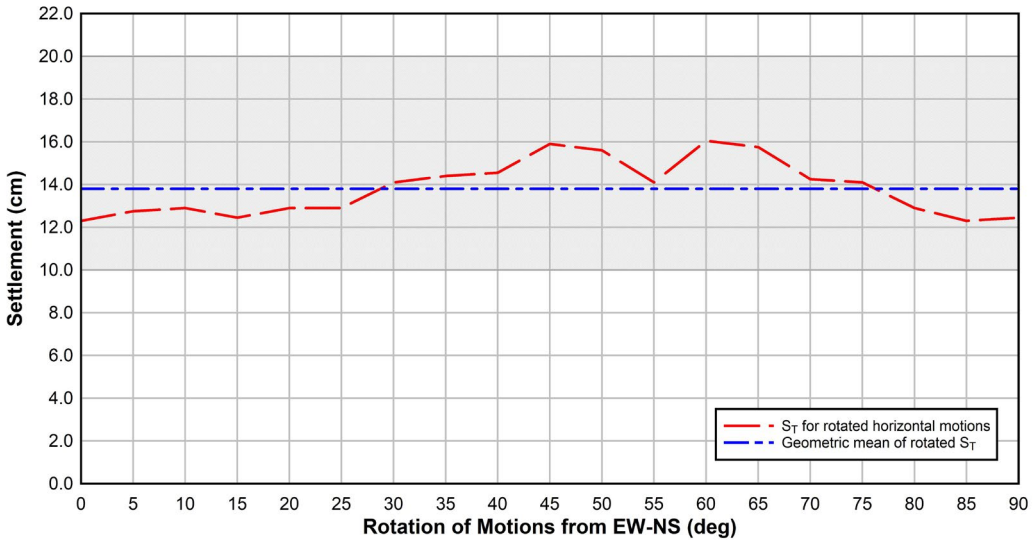

Figure 2: Predicted settlement as a function of ground motion orientation. The shaded region is the range of post-earthquake field observed settlements.

5 CONCLUSIONS

The non-simplified expanded Byrne model was used to evaluate seismic compression at the KKNPP SHA site during the main shock of the 2007, M_w6.6 Niigata-ken Chuetsu-oki, Japan, earthquake. The non-simplified model was used in conjunction with shear strain time histories computed at varying depths in the profile using EQL site response analyses. To assess the influence of the motion orientation of the magnitude of the predicted settlements due to seismic compression, the motions were rotated in 5° increments and the case history was analyzed for each set of motions. The range of predicted settlements is in good accord with post-event observations at the KKNPP site (i.e., predicted: 12.3-16.1 cm vs. observed:10-20 cm). However, this relatively large variation in predicted settlements due to motion orientation highlights the importance of both the absolute amplitude and sequencing of pulses in the load history on predicted magnitude of seismic compression (i.e., the significance of the load-dependent, interaction macro-level fatigue behavior exhibited by the seismic compression phenomenon), which is commonly ignored in computation of the number of equivalent strain cycle relationships used in conjunction with simplified variants of seismic compression models.

ACKNOWLEDGEMENTS

This study is based on work supported by the US Army Engineer Research and Development Center (ERDC) Grant W912HZ-13-C-0035 and U.S. National Science Foundation (NSF) Grants CMMI-1435494, CMMI-1724575, and CMMI-1825189. The authors gratefully acknowledge this funding. Additionally, the authors greatly appreciate the help from Mr. Yusheng (Bear) Jiang, Dr. Oliver-Denzil Taylor, and Professors Jonathan Stewart and Ramin Motamed regarding the KKNPP case history. The ground motion data used in this study belongs Tokyo Electric Power Company, and the distribution license of the data belongs to Japan Association for Earthquake Engineering (JAEE). Finally, any opinions, findings, and conclusions or recommendations expressed in this paper are those of the authors and do not necessarily reflect the views of ERDC, NSF, or JAEE or those that have provided help on this study.

REFERENCES

Boore, D.M. 2005. On pads and filters: processing strong-motion data. *Bulletin of the Seismological Society of America*, Vol 95, 745–750.

Boore, B.M. & Bommer, J.J. 2005. Processing of strong-motion accelerograms: needs, options and consequences, *Soil Dynamics and Earthquake Engineering*, Vol 25, 93–115.

Boore, D.M., Watson-Lamprey, J. & Abrahamson, N.A. 2006. Orientation-independent measures of ground motion. *Bulletin of the Seismological Society of America*, Vol 96(4A) 1502-1511.

Byrne, P. 1991. A cyclic shear-volume coupling and pore pressure model for sand. *Proc., 2nd Int. Conf. on Recent Advances in Geotechnical Earthquake Engineering and Soil Dynamics*, Missouri Univ. of Science and Technology, Rolla, MO, 47–55.

Darendeli, M. 2001. *Development of a new family of normalized modulus reduction and material damping curves*. Ph.D. Dissertation, Dept. of Civil Eng., Univ. of Texas, Austin, TX.

Dobry, R., Ladd, R.S., Yokel, F.Y., Chung, R.M. & Powell, D. 1982. *Prediction of Pore Water Pressure Buildup and Liquefaction of Sands During Earthquakes by the Cyclic Strain Methods*, Building Science Series 138, National Bureau of Standards, U.S. Department of Commerce, U.S. Government Printing Office, Washington, D.C.

Duku, P.M., Stewart, J.P., Whang, D.H. & Yee, E. 2008. Volumetric strains of clean sands subject to cyclic loads. *Journal Geotechnical and Geoenvironmental Engineering*, Vol 134(8), 1073-1085.

Finn, W.D.L. & Byrne, P.M. 1976. Estimating settlements in dry sands during earthquakes. *Canadian Geotechnical Journal*, Vol 13(4), 355–363.

Green, R.A. & Jiang, Y. 2020. Comparison of seismic compression procedure predictions: Case history from Japan. *Proc. 17th World Conference on Earthquake Engineering*, Sendai, Japan, 13-18 September 2020. (*in review*)

Green, R.A. & Lee, J. 2006. Computation of number of equivalent strain cycles: A theoretical framework. *Geomechanics II: Testing, modeling, and simulation*, P. V. Lade and T. Nakai, eds., ASCE, Reston, VA, 471–487.

Green, R.A. & Terri, G.A. 2005. Number of equivalent cycles concept for liquefaction evaluations—Revisited. *Journal Geotechnical and Geoenvironmental Engineering*, Vol 131(4), 477–488.

Kaechele, L. 1963. *Review and analysis of cumulative-fatigue-damage theories*. Memorandum RM-3650-PR, Rand Corporation, Santa Monica, CA.

Kayen, R., Brandenberg, S.J., Collins, B.D., Dickenson, S., Ashford, S., Kawamata, Y., Tanaka, Y., Koumoto, H., Abrahamson, N., Cluff, L. & Tokimatsu, K. 2009. Geoengineering and seismological aspects of the Niigata-ken Chuetsu-oki earthquake of 16 July 2007. *Earthquake Spectra*, Vol 25(4), 777–802.

Kottke, A. & Rathje, E.M. 2009. *Technical Manual for Strata*. PEER 2008/10, Pacific Earthquake Engineering Research Center, University of California at Berkeley, Berkeley, CA.

Jiang, Y., Green, R.A. & Taylor, O.-D. 2020. Expanded Byrne Model for Evaluating Seismic Compression. *Earthquake Spectra*. (*in review*)

Lasley, S. & Green, R.A. 2012. *Evaluating Seismic Compression and Post Liquefaction Settlement at Level-Ground Sites*, Center for Geotechnical Practice and Research (CGPR) Report #69, The Charles E. Via, Jr., Department of Civil and Environmental Engineering, Virginia Tech, Blacksburg, VA.

Lasley, S., Green, R.A., Chen, Q. & Rodriguez-Marek, A. 2016. "Approach for Estimating Seismic Compression Using Site Response Analyses, *Journal Geotechnical and Geoenvironmental Engineering*, Vol 142(6), 04016015.

Lee, J. & Green, R.A. 2017. Number of Equivalent Strain Cycles for Active Tectonic and Stable Continental Regions. *Proc. 19th Intern. Conf. on Soil Mechanics and Geotechnical Engineering*, Seoul, Korea, 17-22 September.

Li, X. S., Wang, Z.L. & Shen, C.K. 1992. *SUMDES: A nonlinear procedure for response analysis of horizontally-layered sites subjected to multi-directional earthquake loading*. Dept. of Civil Engineering, Univ. of California, Davis, CA.

Martin, G.R., Finn, W.D.L. & Seed, H.B. 1975. Fundamentals of liquefaction under cyclic loading. *Journal Geotechnical Engineering Division*, Vol 101(GT5), 423–438.

Menq, F.Y. 2003. *Dynamic properties of sandy and gravelly soils*, Ph.D. Dissertation, Dept. of Civil Eng., Univ. of Texas, Austin, TX.

Motamed, R., Stanton, K., Almufti, I., Ellison, K. & Willford, M. 2016. Improved approach for modeling nonlinear site response of highly strained soils: Case study of Service Hall Array in Japan. *Earthquake Spectra*, Vol 32(2), 1055-1074.

Nie, C.-X., Chen, Q.-S., Gao, G.-Y. & Yang, J. 2017. Determination of seismic compression of sand subjected to two horizontal components of earthquake ground motions. *Soil Dynamics and Earthquake Engineering*, Vol 92, 330-333.

Pyke, R., Seed, H.B. & Chan, C.K. 1975. Settlement of sands under multidirectional shaking. *Journal of Geotechnical Engineering*, Vol 101(4), 379-398.

Seed, H.B. & Silver, M.L. 1972. Settlement of dry sands during earthquakes, *Journal of Soil Mechanics and Foundation Division*, Vol 98(SM4), 381–397.

Silver, M.L. & Seed, H.B. 1971. Volume changes in sands during cyclic loading, *Journal of Soil Mechanics and Foundation Division*, Vol 97(SM9), 1171–1182.

Skempton, A.W. 1986. Standard penetration test procedures and the effects in sands of overburden pressure, relative density, particle size, aging, and overconsolidation. *Geotechnique*, Vol 36(3), 425-447.

Stewart, J.P., Smith, P.M., Whang, D.H. & Bray J.D. 2004. Seismic compression of two compacted earth fills shaken by the 1994 Northridge earthquake. *Journal of Geotechnical and Geoenvirontal Engineering*, Vol 130(5), 461-476.

Yee, E., Stewart, J.P. & Tokimatsu, K. 2011. *Nonlinear site response and seismic compression at vertical array strongly shaken by 2007 Niigata-ken Chuetsu-oki earthquake*. Rep. No. 2011/107, Pacific Earthquake Engineering Research Center, Univ. of California, Berkeley, CA.

Yee, E., Stewart, J.P. & Tokimatsu, K. 2013. Elastic and large-strain nonlinear seismic site response from analysis of vertical array recordings. *Journal of Geotechnical and Geoenvironmental Engineering*, Vol 139(10), 1789–1801.

Yee, E., Duku, P.M. & Stewart, J.P. 2014. Cyclic volumetric strain behavior of sands with fines of low plasticity. *Journal of Geotechnical and Geoenvironmental Engineering*, Vol 140(4), 04013042.